

## The Effects of Hydrogen Peroxide and Deposition Temperature on the electrodeposited Zinc Oxide Film

Jee-Ray Wang<sup>1</sup>, Miao-Ju Chuang<sup>1</sup>, Yuan-Gee Lee<sup>1,\*</sup>, Der-Wei Chen<sup>2</sup>, Kung-Hsu Hou<sup>2,\*</sup>

<sup>1</sup> Department of Automation Engineering and Institute of Mechatronic Systems, Changhua, Taiwan.

<sup>2</sup> Department of Power Vehicle and Systems Engineering, Chung Cheng Institute of Technology, National Defense University, Taoyuan, Taiwan.

\*E-mail: [yglee@cc.ctu.edu.tw](mailto:yglee@cc.ctu.edu.tw), [khou@ndu.edu.tw](mailto:khou@ndu.edu.tw), [khoucloud@gmail.com](mailto:khoucloud@gmail.com)

Received: 22 May 2016 / Accepted: 19 August 2016 / Published: 6 September 2016

---

Zinc oxide (ZnO) film was successfully electrodeposited on a substrate of indium-tin oxide (ITO) by reduction of zinc chloride. It was found that both the content of hydrogen peroxide and the electroposition temperature dominated the microstructure variation and its optical properties. The morphology of ZnO film revealed different growth mechanism, i.e. film with large flake-like crystal without H<sub>2</sub>O<sub>2</sub> in contrast to the fine surface with H<sub>2</sub>O<sub>2</sub> included. During electrodeposition, organometallic compound, Zn<sub>5</sub>(OH)<sub>8</sub>·H<sub>2</sub>O, co-precipitated on the electrode which was depressed by hydrogen peroxide (H<sub>2</sub>O<sub>2</sub>) and burn-out in an annealing process. Besides, H<sub>2</sub>O<sub>2</sub> could result of crystal defects in ZnO to produce new doped-energy level, E<sub>d</sub>, and thus reduce the photon energy as a red-shift. On the other hand, the under substrate could affect the transmittance to induce blue-shift caused by the lattice distortion at the interlayer, ZnO/ITO.

---

**Keywords:** zinc chloride, hydrogen peroxide, microstructure variation, doped-energy level

### 1. INTRODUCTION

Solar energy provides the earth with great power, 1.73x10<sup>14</sup> kW all the time. Ironically, the earth couldn't keep it owing to its dissipating in the atmosphere; therefore, the topic of energy conservation always plays an important role nowadays. One of the most critical issues to determine the sustainable development is to store energy with a reservoir which could save and release energy fluently. Solar cell is one of the energy-saving equipment in which the solar energy is transformed into electrical power by way of a reverse process of ambipolar recombination. In solar cell the photoactive layer is a kind of hybrid films composed of an inorganic mesoporous matrix with a large bandgap semiconductor, e.g. TiO<sub>2</sub> [1] and ZnO [2], responsible of sensitization.

Zinc oxide is one of the most promising oxide semiconductors because of its excellent electrical, good optical and acoustic characteristics. It was applied in many fields such as field-emission displays, transparent conducting windows in solar cells, and gas sensors [3]. Zinc oxide is an n type II–VI compound semiconductor with a bandgap of 3.3 eV, and a Wurtzite crystal structure,  $a=0.325$  nm and  $c=0.512$  nm. Zinc oxide film is usually prepared by Physical Vapor Deposition (PVD) [4] or Chemical Vapor Deposition (CVD) to obtain a good crystalline quality[5]. However, these two kinds of technologies requires an environment with vacuum and high temperature which costs high for the investor. In contrast, electrochemical deposition is a simple and un-expensive process which was used in industry extensively. Many researchers devoted themselves to the preparation with aqueous solutions and they announced many advantages [6-8]. Pauporte and his co-worker researched the electrodeposition of zinc oxide but no study related to conductivity was found in his research[9]. Wang and his co-workers researched structure of ZnO; nevertheless, optoelectronic properties were not taken into account in their paper [10].

This paper researches the microstructure related to its optoelectronic characteristics. We also investigated how the hydrogen peroxide prevailed against hydroxide by way of competing active sites. Because a kind of organometallic compound appeared as an intermediate in this research, we investigated how the  $H_2O_2$  depressed the intermediate and hence inhabited the growth of ZnO layer. We also related the transmission spectra to the lattice distortion of ZnO layer, one criterion to result of spectra shift in the lamination process.

## 2. EXPERIMENTAL DETAILS

### 2.1. Preparation of the zinc oxide film

Slices of coated indium-tin oxide with dimension  $2\text{cm}\times 3\text{cm}$  were prepared as the substrates which experienced cleaning with acetone and isopropanol in turn ultrasonically. These pieces were dried in oven at  $80^\circ\text{C}$  for 15 minutes. A stock solution including potassium chloride 0.05 M (BASF Co.); zinc chloride 0.25 M, 0.075 M and 0.125M (BASF Co.); and hydrogen peroxide 0.005 M and 0.05 M (BASF Co.) was prepared to serve as deposition solution. An electro-deposition system with three electrodes, ITO glass as working, platinum as counter and saturated camel electrode as reference, was applied in the deposition solution. A potentiostat (SP-150, Biologic Co.) was employed in this research. After cyclic voltammographic searching, the applied voltage was set from  $-0.7\text{V}$  to  $-1.2\text{V}$ . The deposition temperature ranged from room temperature to  $65^\circ\text{C}$ . After deposition, the slices were annealed in the furnace (Model BF51442C, Lindberg Co.) at  $500^\circ\text{C}$  for 2 hours.

### 2.2. Characterization of the deposited zinc oxide films

Scanning electron microscope (Hitach Co., S-300 SEM) equipped with energy dispersive spectrum (Horiba Co.) and Atomic force microscope (Digital Co., AFM) were applied to double-check the morphology of the deposited films. X-ray diffractometer (Rigaku Co. XRD) was applied to identify

the phase of the deposited films. Ultra-visible spectroscope (Bruker Co. UV-Vis) was applied to measure its emission spectrum. Four point probe (4PP, KLA-Tencor/Prometrix Co.) was employed to measure their resistivity.

### 3. RESULTS AND DISCUSSION

#### 3.1. Electrochemistry

Hydrogen peroxide prevailed against hydroxide when they competed the active sites in reduction process. Figure 1 showed a series of cyclic voltammograms for the variation of  $\text{H}_2\text{O}_2$  concentration in the deposition solution.

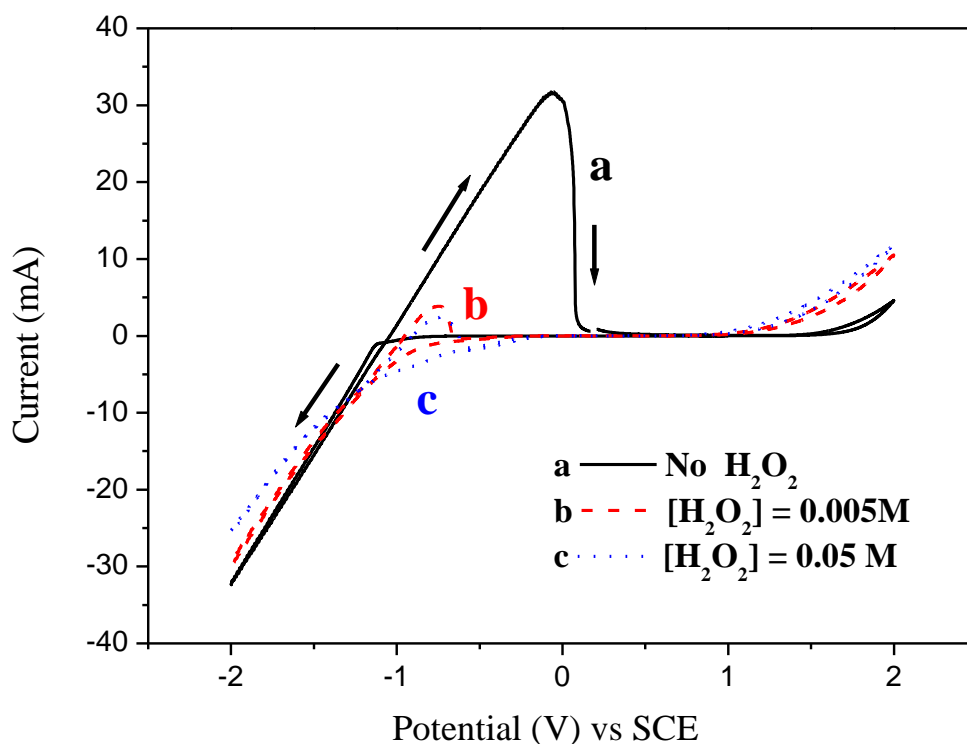


**Figure 1.** Cyclic voltammograms for different concentration of hydrogen peroxide inside the electrodeposition solution. The scan rate was 10 mV/min.

Focus on the peak labeled “a” in which a large broadened wave with positive current appeared to reveal a wide voltage window for decomposing pure  $\text{H}_2\text{O}$ . The reduction current aroused from the electron transfer in electrolyzing  $\text{H}_2\text{O}$ , which is expressed as in the following



In contrast to peak “a”, the reduction current no more showed a large wave in which little amount of  $\text{H}_2\text{O}_2$ , 0.005 M, was blended as shown in peak “b”. The peak current was further shrunk

appreciable to peak “c” with amplifying  $\text{H}_2\text{O}_2$  to 10 times of former concentration, 0.05 M. Because  $\text{H}_2\text{O}_2$  is a strong oxidant possessing a strong chemical potential to occupy more active sites, it could also release electrons as reduction current.

A competing relationship between the  $\text{H}_2\text{O}$  and  $\text{H}_2\text{O}_2$  molecules was constructed on the working electrode. However, not only does the kinetics of electron transfer depend on the chemical potential of oxidant but it depends on the migrating speed of the diffusing ions. It is due to the oxidant,  $\text{H}_2\text{O}_2$ , of which the molecule size is larger than  $\text{H}_2\text{O}$ . Excess  $\text{H}_2\text{O}_2$  molecules could result in block on exchanging reactive  $\text{H}_2\text{O}_2$  molecules; therefore, even 10 times of  $\text{H}_2\text{O}_2$  concentration resulted of appreciable reduction current in Fig.1(c).

Moss-Burstein shift occurred in this study. Pouporte and his coworker electrodeposited zinc oxide by employing an alternative electrolyte, perchlorate, instead of chlorate and they obtained similar cyclic voltammograms labeled with no hydrogen peroxide and 2.5 mM hydrogen peroxide inside.[11,12] In their former voltammogram, three reduction peaks appeared to show a catalytic energy level of electro-activation for electron transfer. It can be inferred that, except for the water reduction in Eq.(1), two more reduction reaction were illustrated as follows



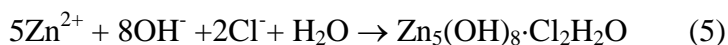
and



Note that this reduced zinc was too active to keep an element state; therefore, it immediately oxidized with solution-contained oxygen molecule in a manner of homogeneous nucleation with large grains and rough morphology. In the other voltammogram, i.e. 2.5 mM hydrogen peroxide inside, these three peaks shrunk into a small peak in which hydrogen peroxide was blended as support electrolyte. The hydrogen peroxide not only play a strong oxidation reagent to keep the reactants in high valance but itself was prone to decomposing into hydroxide ions ready for electro-catalyzing as a complex,  $\text{Zn}_5(\text{OH})_8 \cdot \text{Cl}_2\text{H}_2\text{O}$ , in the following way



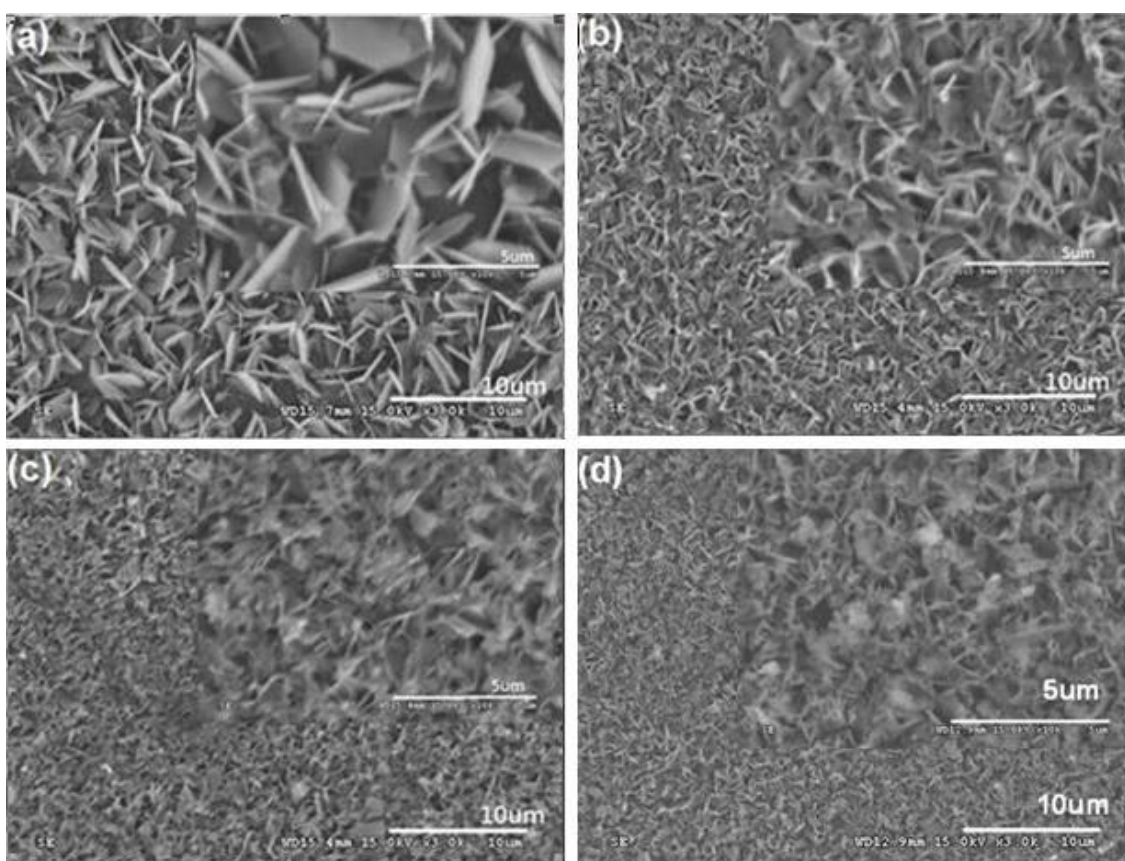
and



In their experiment the specific additive electrolyte, perchlorate, could inhabit high solubility of complex in Eq.(5), and thus the complex had enough space to proceed the succeeding diffusion-controlled crystallization of zinc oxide.[13] They obtained nano-scaled crystal with conduction energy keeping at a close energy level, i.e. a uniform energy gap. In contrast, a different way of crystallization was found when the perchlorate was replaced with chlorate to serve as the electrolyte in this study. Chloride ion not only allowed high solubility of complex in the solution but its high absorbing force could occupy the nucleation sites of zinc oxide.[14] High solubility of complex could result of blocking purge patch of by-product from complex to ZnO; nevertheless, under finite nucleation sites, the film growth mainly relied on coarsening or Oswald ripening.[15] The deposited ZnO crystal not only enclosed complex-rich inclusion but it grew without texture, i.e. defects upon the crystal. Based on the energy level of well-crystallized ZnO, these defective or amorphous ZnO could stack excess doping energy level to extend the conduction band with a wider energy band gap.[16] A Moss-Burstein shift, therefore, occurred and it resulted of blue-shift in the transmission spectrum.[17]

### 3.2. Morphology Investigation

Hydrogen peroxide facilitated surface diffusion for hydroxide ion,  $\text{OH}^-$ , on the substrate. Figures 2 showed the morphology of ZnO film for different concentration of hydrogen peroxide in the solution. In Fig.2(a) the film presented a rough feature with large flake-like crystal in contrast to the fine surface as shown in Fig.2(b). The morphology became dense when the concentration was increased to 10 times, 0.05 M, as shown in Fig.2(c). This demonstrates a distinct kinetics in which a homogeneous nucleation performed on condition of no  $\text{H}_2\text{O}_2$  to show a rough surface; nevertheless, an inhomogeneous nucleation occurred to result in fine feature. It is due to the inhomogeneous nucleation which is related to the surface-diffused intermediates,  $\text{OH}^-$ , in Stern layer. Though a great amount of  $\text{H}_2\text{O}_2$  was introduced in the solution, the number of  $\text{H}_2\text{O}_2$  molecules allowed to approach electrode was saturated as mentioned in the previous paragraph.



**Figures 2.** The morphology for different concentration of hydrogen peroxide in the deposition solution, (a) no hydrogen peroxide, (b) 0.005 M, (c) 0.05 M and (d) 0.05 M post-annealing.

Hydrogen peroxide possessed an effect on depressing the formation of organometallic compound. Figure 3(a) showed the x-ray diffraction patterns of as-received deposited layer for with/without  $\text{H}_2\text{O}_2$  in the solution. Note that, expect for the ITO peaks and a ZnO (101) peak, all the rest were identified to be organometallic compound,  $\text{Zn}_5(\text{OH})_8 \cdot \text{H}_2\text{O}$ . The organometallic compound was also found in Peulon's and Lincot's reports in which basic salts often formed at higher concentration of  $\text{Zn}^{2+}$ . [13] In Fig.3(a), broadened peaks appeared in the pattern labeled as " $\text{H}_2\text{O}_2$

0.005M” and “H<sub>2</sub>O<sub>2</sub> 0.05M” to compare with the sharp pattern labeled as “No H<sub>2</sub>O<sub>2</sub>”. This indicates that coarse grains with a lot of crystal orientations related to the organometallic, e.g. (006), (015), (017) and (205), formed in the solution without H<sub>2</sub>O<sub>2</sub> as matched with the morphology in Fig.2(a). On the contrary, most of the organometallic peaks disappeared on the pattern with H<sub>2</sub>O<sub>2</sub> as matched with the morphology in Figs.2(b) and 2(c). This confirms a depress effect on the textual formation of the organometallic compound in case of H<sub>2</sub>O<sub>2</sub> presenting. The organometallic compound was apt to transform into ZnO through a burn-out process to eliminate the organic components as shown in Fig.3(b).

Hydrogen peroxide could result of crystal defects in ZnO to produce new doped-energy level, E<sub>d</sub>, and thus reduce the photon energy. Though hydrogen peroxide could inhabit the grain growth, the fine morphology in Fig.2(b) and (c) could contain some defects, i.e. vacancy or interstitial atoms inside, to establish new doped energy levels above the valance band.

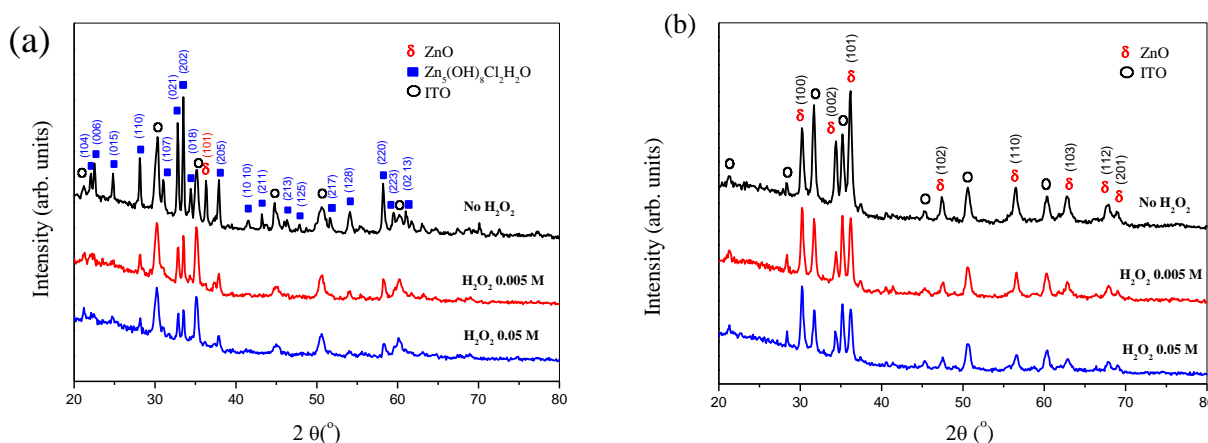


Figure 3. The x-ray diffraction patterns of ZnO films (a) before annealing and (b) after annealing.

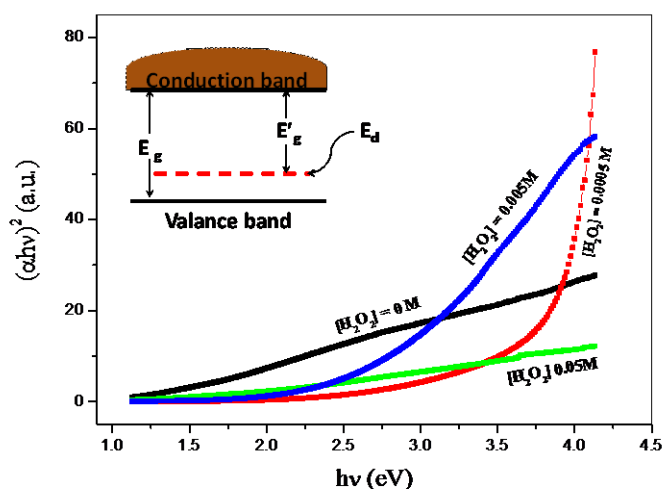
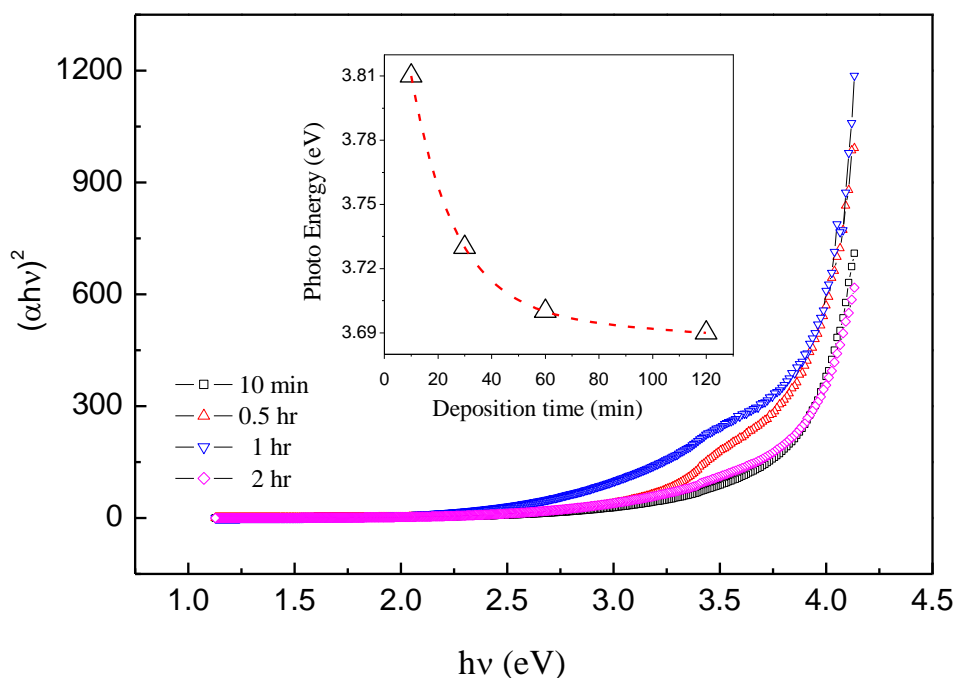


Figure 4. Tauc’s plot for different concentration of hydrogen peroxide. The inset is the schematic plot of the jump level for electrical carriers in which E<sub>g</sub>, E’<sub>g</sub> and E<sub>d</sub> represents the energy gap for perfect crystal, energy gap for imperfect crystal and the new doped energy level.

With the increase of  $\text{H}_2\text{O}_2$  concentration, the doped energy level could extend to be a band and the original energy gap,  $E_g$ , shrunk as  $E'_g$  as shown in Fig.4. When the stimulated electrons jumped back to the new doped energy band, photon emitted with less energy, i.e. red-shift, e.g. 3.68 eV for 0.0005 M  $\text{H}_2\text{O}_2$  to 2.61 eV for 0.005 M  $\text{H}_2\text{O}_2$ .



**Figure 5.** Tacu's plot for different deposition time in which the inset was obtained from the abscissa intercepts of the curve extrapolating.

Lattice distortion of ZnO could result of blue shift in the lamination process. Figure 5 showed the specular transmission spectra for the deposited layers with different deposition time, 10 min, 1hr and 2 hr. After extrapolating to abscissa,  $h\nu$ , the intercepts revealed energy gaps, 3.69, 3.75 and 3.81 eV, for 10 min, 1hr and 2 hr, respectively. Because the deposited layer was apt to be compliant with the lattice of under-layer, ITO, lattice distortion could occur in the interlayer of ZnO/ITO. With elapsed deposition time, the lattice distortion reduced and the texture formed. We thus conclude that the change of the energy gap, blue shift, resulted from the lattice distortion of ZnO. Besides, the size of deposited ZnO contributes the blue shift due to the short deposition time inducing fine grains and blue-shift.[18] Extremely ZnO crystal presented a deep level or trap-state emission, which is related to structure defects.[19] The longer the elapsed time the more well the ZnO crystallized and thus the closer to the theoretical energy gap, 3.37 eV.

High deposition temperature facilitates devitrification to reduce transmittance of the ZnO film. Figure 6 showed the transmittance at different temperature. Note that the transmittance decreased with the increase of temperature. Because the ZnO film became well-crystallized at high deposition temperature, the characteristics of amorphous-like, i.e. glass transparency, no more appeared.[20-21] Instead, well-crystallized growth devitrified ZnO film to reduce its transmittance.

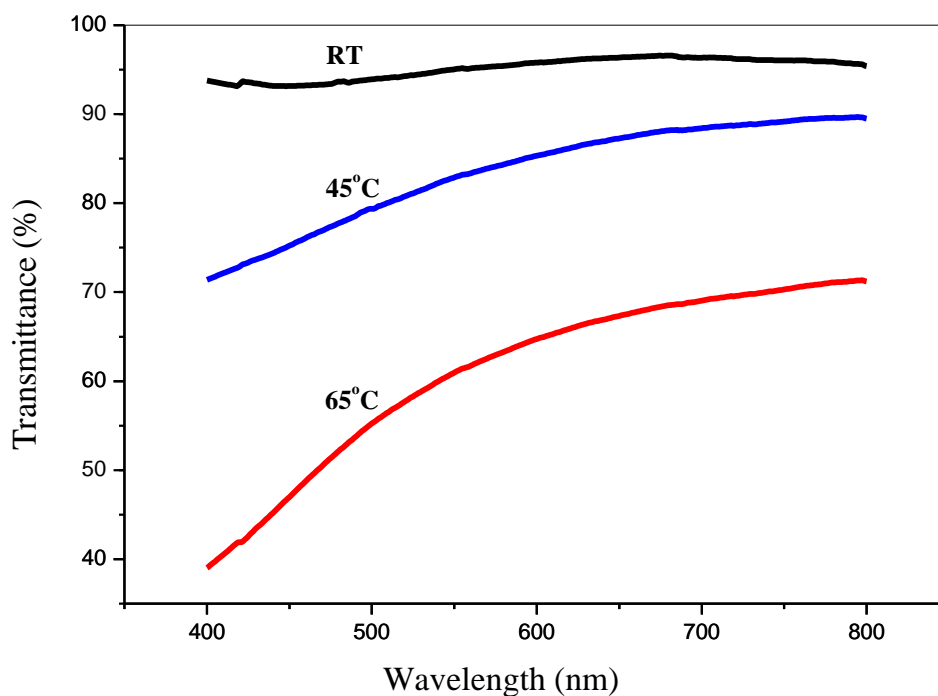


**Figure 6.** The transmittance with different deposition temperature as a function of wavelength.

#### 4. CONCLUSION

From cyclic voltammograms, we deduced that the competition of diffusion for  $\text{H}_2\text{O}_2$  and  $\text{H}_2\text{O}$  molecules resulted of the magnitude of the reductive current. Though the hydrogen peroxide molecule was a stronger reductive than  $\text{H}_2\text{O}$ , the large size of  $\text{H}_2\text{O}_2$  molecule blocked the diffusional pathway for reactant to reach working electrode. Even high  $\text{H}_2\text{O}_2$  concentration couldn't increase considerable reduction current. .

The morphology of ZnO film demonstrated distinct growth mechanism in which the film presented a feature of large flake-like crystal without  $\text{H}_2\text{O}_2$  in contrast to the fine surface with  $\text{H}_2\text{O}_2$  included. The former feature, rough surface, possessed a large specific area to provide the reactive intermediates,  $\text{OH}^-$ , with more electro-active sites than that of the latter feature, fine surface. More electro-active sites produced more number of electron transfer and thus high reductive current.

During the process of electrodeposition, a kind of organometallic compound,  $\text{Zn}_5(\text{OH})_8\cdot\text{H}_2\text{O}$ , co-precipitated on the electrode. According to the identification of x-ray diffraction patterns, hydrogen peroxide could depress the formation of the organometallic compound which was apt to transforming into ZnO by way of a burn-out process. Because the deposited layer was apt to be compliant with the lattice of under-layer, ITO, lattice distortion occurred in the interlayer of ZnO/ITO. With elapsed deposition time, the lattice distortion reduced and the texture formed to shift the transmission spectra toward the short wavelength, i.e. blue shift. We thus concluded that lattice distortion of ZnO resulted

of blue shift in deposition. Besides, we found that high deposition temperature could facilitate crystallize and devitrificate the film to reduce transmittance of the electrodeposited ZnO film.

#### ACKNOWLEDGMENTS

We thank the financial support by the Chienkuo Technology University under Grant No. CTU-103-RP-AE-002-002-A) and CTU-103-RP-AE-003-003-A.

#### References

1. B. O'Reagan and M. Grätzel, *Nature.*, 353 (1991) 737.
2. G. Redmond, D. Fitzmaurice and M. Graetzel, *Chem. Mater.*, 6 (1994) 686.
3. K. -S. Weißenrieder and J. Müller, *Thin Solid Films.*, 300 (1997) 30.
4. L. Dai, X. L. Chen, W. J. Wang, T. Zhou and B. Q. Hu, *J. Phys. Condens. Matter.*, 15 (2003) 2221.
5. B.Y. Geng, T. Xie, X. S. Peng, Y. Lin, X. Y. Yuan, G. W. Meng and L. D. Zhang, *Appl. Phys. A.*, 77 (2003) 363.
6. Th. Pauporté, T. Yoshida, A. Goux and D. Lincot, *J. Electroanal. Chem.*, 534 (2002) 55.
7. Z. Yu, X. Jia, J. Du and J. Zhang, *Solar. Energy. Mater. Solar. Cells.*, 64 (2000) 55.
8. J Lee, H Varela, S Uhm and Y Tak, *Electrochem. Commun.*, 2 (2000) 646.
9. Th. Pauporté and D. Lincot, *J. Electrochem.*, 148 (2001) C310.
10. Y. L. Wang, A. Y. Ouslim and G. Y. Wang, *Microelectron. J.*, 36 (2005) 625.
11. Pauporte, T. and D. Lincot, *J. Electrochem. Soc.*, 148 (2001) C310
12. Pauporte, T. and D. Lincot, *J. Electroanal. Chem.*, 517 (2001) 54
13. S. Peulon and D. Lincot, *J. Electrochem. Soc.*, 145 (1998) 864
14. G. Hodes, *Isr. J. Chem.* 33 (1993) 95
15. C. Pacholski, A. Kornowski and H. Weller, *Angew. Chem Int. Edit*, 41, Issue 7, 2002, 1188–1191
16. S. T. Tan, B. J. Chen, X. W. Sun, a and W. J. Fan, *J. Appl. Phys.* 98 (2005) 013505
17. B. E. Sernelius, K.-F. Berggren, Z.-C. Jin, I. Hamberg, and C. G. Granqvist, *Phys. Rev. B* 37 (1998) 10244
18. L. Brus, *J. Phys. Chem.*, 90 (1986) 2555.
19. X. Y. Kong, Y. Ding, R. Yang, Z. L. Wang, *Science* 303 (2004) 1348.
20. R. Rossetti, S. Nakahara and L. E. Brus, *J. Chem. Phys.*, 79 (1983) 1086.
21. A. Goux, T. Pauporte, J. Chivot and D. Lincot, *Electrochimica. Acta.*, 50 (2005) 2239.